

Current Density and Reversible Magnetization of $\text{HgBa}_2\text{Ca}_2\text{Cu}_3\text{O}_x$ Superconductors Containing Randomly Oriented Columnar Defects

J. R. Thompson,^{a,b} J. G. Ossandon,^c L. Krusin-Elbaum,^d H. J. Kim,^b D. K. Christen,^a K. J. Song,^b K. D. Sorge,^b and J. L. Ullmann^e

^a Oak Ridge National Laboratory, Oak Ridge, Tennessee, 37831-6061 USA

^b Department of Physics, University of Tennessee, Knoxville, Tennessee 37996-1200 USA

^c Department of Engineering Sciences, University of Talca, Curico, Chile

^d IBM Watson Research Center, Yorktown, New York, 10598 USA

^e Los Alamos National Laboratory, Los Alamos, New Mexico, 87545 USA

(29 April 2002)

Bulk polycrystalline $\text{HgBa}_2\text{Ca}_2\text{Cu}_3\text{O}_x$ materials were irradiated with 0.8 GeV protons to form randomly oriented columnar defects, by induced fission of Hg-nuclei. Proton fluences from 0 to $35 \times 10^{16} \text{ cm}^{-2}$ were used to install defects with area densities up to a “matching field” of 3.4 Tesla. Studies were conducted on the dependence of the equilibrium magnetization and the intragrain persistent current density on temperature and applied magnetic field, at various defect densities. The magnetization was modeled using London theory with the addition of vortex-defect interactions.

Corresponding author: James R. Thompson Oak Ridge National Laboratory PO Box 2008 Oak Ridge, TN 37831-6061 USA Phone: 865-574-0412; fax: 865-574-6263; email: JRT@UTK.EDU

I. INTRODUCTION

For strong pinning of vortices in high- T_c superconductors, some form of correlated disorder generally is most effective. Most widely studied have been columnar defects, which typically are formed by irradiation with energetic heavy ions; such particles are highly ionizing and create tracks of amorphous material along their path.¹ Many morphologies have been investigated, ranging from the familiar parallel tracks to inclined defects, crossed arrays with “designer splay,” etc. One problem with heavy ions is their limited range, typically a few tens of micrometers. To overcome the limited range of heavy ions, Krusin-Elbaum et al.² demonstrated an indirect formation of columnar defects using deeply penetrating 0.8 GeV protons. In this process, an incident proton is absorbed by a heavy nucleus (Hg) within the material and excites it into a highly energetic state. As a consequence, the nucleus breaks into two particles with similar mass, each having ~ 100 MeV energy. The fission fragments form randomly oriented columnar defects (CD’s) deep within the superconductor. In a different approach to create pins deep inside a material, Weinstein and coworkers have created CD’s by introducing ^{235}U as a dopant into the superconductor, which is induced to fission by irradiation with thermal neutrons.³

Vortex pinning by proton-generated fission defects was first demonstrated in Bi-cuprate materials.^{2,4} In fact, the proton-based fission process is generally applicable in cuprate superconductors that contain a sufficient density of heavy nuclei.⁵ High- T_c materials containing randomly oriented CD’s exhibit a variety of interesting physical phenomena, e.g., temperature independent quantum tunneling of vortices in Bi-2212 materials.⁶ In studies of a

series of Hg-cuprates containing 1, 2, and 3 adjacent CuO layers, it was shown⁷ that sufficiently high superconductive anisotropy can lead to a rescaling of the splayed landscape of random CD’s. As a consequence, the pinning array and the applied field are ‘refocused’ toward the crystalline c -axis, even in polycrystalline materials. This is a useful feature that we will use when interpreting present studies of the equilibrium magnetization.

In this paper, we describe how the addition of random CD’s changes the superconductive properties of $\text{HgBa}_2\text{Ca}_2\text{Cu}_3\text{O}_x$ superconductors. Specific topics include the intragrain persistent current density J , as obtained from the magnetization; establishment of the optimum defect density; and analysis of the changes in the mixed state reversible (or equilibrium) magnetization resulting from interactions between vortices and randomly oriented columnar defects.

II. EXPERIMENTAL ASPECTS

Samples for study were bulk polycrystalline $\text{HgBa}_2\text{Ca}_2\text{Cu}_3\text{O}_x$ materials (Hg-1223) containing sets of 3 adjacent oxygen-copper layers. Small pieces, typically 30 mg mass and ~ 1 millimeter thickness, were all cut from the same pellet. The samples were irradiated at room temperature in air with 0.8 GeV protons at the Los Alamos National Laboratory. Proton fluences ϕ_p were 0, 1.0, 3.2, 10, 19, and 35×10^{16} protons/cm², as determined from the activation of Al dosimetry foils. The resulting density of fission events is $N/V = \phi_p \sigma_f n_{\text{Hg}}$. Here n_{Hg} is the number density of Hg nuclei and $\sigma_f = \sim 80$ millibarns is the cross-section for inducing a prompt fission of Hg nuclei. Each fission produces one CD, so N/V is

the volume density of defects, also. One can convert this into an approximate area density of CD's by multiplying by the track length $\sim 8 \mu\text{m}$, and the area density can be reexpressed in units of a matching field B_Φ by multiplying by the flux quantum Φ_0 . Resulting values for the defect density are $B_\Phi = 0, 0.1, 0.3, 1.0, 1.9,$ and 3.4 Tesla, respectively. The fission process is random in direction, giving randomly oriented CD's. Transmission electron microscopy (TEM) studies of both Bi-2212 and Hg-cuprates⁸ have demonstrated the presence of randomly oriented columnar defects in these high- T_c materials.

The superconductive properties of the virgin and processed samples were investigated magnetically. A SQUID-based magnetometer (model Quantum Design MPMS-7), equipped with a high homogeneity 7 T superconductive magnet, was used for studies in the temperature range 5–295 K, in applied fields to 6.5 T. The superconductive transition temperatures T_c were measured in an applied field of 4 Oe (0.4 mT) in zero-field-cooling (ZFC) and field-cooling (FC) modes. The resulting values for the onset temperature T_c are 133, 134, 132.3, 132, 131, and 129.3 K, respectively. Values for the Meissner (FC) fraction $-4\pi M/H$ lie in the range of 40–50%, except at the highest fluence where the fractional flux expulsion was 29%.

The isothermal magnetization M was measured as a function of applied magnetic field. Below T_c and below the irreversibility line, the magnetization was hysteretic due to the presence of intragrain persistent currents. From the magnetic irreversibility $\Delta M = [M(H \downarrow) - M(H \uparrow)]$, the persistent current density J was obtained using the Bean critical state relation $J \propto \Delta M/r$, where $r \approx 4 \mu\text{m}$ is the mean grain radius. Measurements of the background magnetization in the normal state above T_c were used to correct the data in the superconducting state, in order to obtain the equilibrium magnetization M_{eq} . Above the irreversibility line where $\Delta M = 0$, this process yields M_{eq} directly; near the irreversibility line where ΔM is small, we obtain M_{eq} from the (background-corrected) average magnetization $[M(H \downarrow) + M(H \uparrow)]/2$, as illustrated later.

III. EXPERIMENTAL RESULTS

We begin with a discussion of the effects of randomly oriented columnar defects on the irreversible properties of the Hg-1223 superconducting materials. The addition of correlated disorder increases the pinning of vortices, often quite significantly. An example is contained in Fig. 1, which shows the magnetization $M(H)$ at 60 K vs magnetizing field H , for various defect densities. With increasing fluence, the “hysteresis loops” increase in width and become symmetric about the $M = 0$ axis. (The asymmetry for the virgin sample, coupled with the fact that the decreasing field branch lies near the $M = 0$ axis, sug-

gests that surface barriers^{9–11} contribute to the observed hysteresis in this case. It is interesting to note that a relatively low dosage of CD's, $B_\Phi = 0.1$ T, symmetrizes the $M(H)$ loop significantly; in particular, the magnitude of M in the decreasing field branch is much larger. These features imply that the addition of CD's suppresses the surface barrier, as recently discussed by Koshelev and Vinokur.¹²)

Using the Bean model, one may obtain the persistent current density $J(H, T)$. For these weakly linked polycrystalline materials, the magnetization reflects the *intragranular* current density. Some results of this analysis are shown in Fig. 2 and Fig. 3 as plots of J versus temperature T , in applied fields of 0.1 and 1 Tesla, respectively. The enhancement in J is modest in low fields; this can be attributed to the presence in the virgin sample of both naturally occurring defects that provide some pinning and the likely influence of surface barrier effects, as already noted. In higher fields, the contribution of the random CD's is more apparent and J is enhanced by about an order-of-magnitude. For high- T_c materials with these angularly dispersed defects, one generally achieves the maximum J at some defect density B_Φ near 0.2–2 T. This optimization is shown by the insets in Figs. 2 and 3. For an applied field of 0.1 T (Fig. 2 inset), J at 100 K is largest for $B_\Phi = 0.1$ –0.3 T. For the second example with a field of 1 T (Fig. 3 inset), J at 60 K is largest for B_Φ near 2 T. Qualitatively, the optimum defect density in each case is comparable with the vortex density, i.e., about $2\times$ larger. At higher defect densities, J decreases. This may be due in part to the presence of additional CD's that help to initiate the hopping of vortices to nearby empty pinning sites. A second, potential influence is a suppression of T_c ; however, the change in T_c is small and these measurements are far from T_c , so this contribution is expected to be small. A third and sizable effect is an irradiation-induced suppression of the vortex line energy and pinning energy, due to changes in the London penetration depth; this will be discussed in a following section. The optimum defect density depends weakly on the temperature as well.

Next we consider the equilibrium magnetization in the mixed state. Figure 4 illustrates the method used to obtain M_{eq} by plotting the background-corrected experimental magnetization for the virgin material (open squares) versus applied magnetic field $\mu_0 H$ on a logarithmic scale. The closed symbols show the average M , which provides a very good approximation to M_{eq} when the hysteresis is small. The solid line is a fit to conventional London theory, which provides that M_{eq} is directly proportional to $(1/\lambda_{ab}^2) \times \ln(\beta B_{c2}/H)$, where λ_{ab} is the in-plane London penetration depth, β is a constant of order unity, and B_{c2} is the upper critical field.¹³ The straight line fit in Fig. 4 shows that the London $\ln(H)$ logarithmic variation describes the field dependence well. Results for M_{eq} in the virgin Hg-1223 material at other temperatures are presented in Fig. 5. One sees from the linear regression lines that the London field dependence is followed

over a wide range of fields and temperatures. Deviations from linearity occur at low fields when H approaches H_{c1} where simple London theory is not valid, and at low temperatures where the materials are sufficiently hysteretic that the averaging procedure illustrated in Fig. 4 is not valid. The slopes of the curves in Fig. 5 provide values for the London penetration depth $\lambda_{ab}(T)$ in the virgin material. These results will be compared and contrasted with values deduced for the irradiated Hg-1223.

We now address the question of how the addition of randomly oriented columnar defects modifies the equilibrium magnetization in the mixed state. The qualitative effects of the CD's are illustrated in Fig. 4, which includes data for M_{eq} at 77 K for irradiated samples with defect densities $B_{\Phi} \approx 1.0$ and 3.4 T. Comparing these data with the virgin curve shows that the CD's reduce the magnitude of the equilibrium magnetization considerably, especially at lower fields. In addition, they generate a pronounced deviation from the "standard" London field dependence, giving M_{eq} an "S"-like dependence on field. This "anomalous" behavior has been observed previously in cuprates containing *parallel* columnar defects formed by 5.8 GeV Pb-ions, in thallium-based single crystals¹⁴; in Bi-2223 tapes¹⁵; and in Bi-2212 single crystals.^{16,17}

These changes in the equilibrium magnetization have been attributed to magnetic interactions between the vortex lattice and the columnar defects. By occupying a pinning site, a vortex gains pinning energy. This reduction in system energy must exceed the energy increase arising from direct intervortex repulsion when a vortex is displaced from its natural position in the lattice to a particular columnar defect. For a defect geometry with parallel tracks that have a Poisson distribution of separations, Wahl et al.¹⁴ obtained an expression for M_{eq} that describes reasonably well the S-shaped field dependence in Tl-cuprate crystals containing parallel CD's.

In the Hg-cuprates investigated here, one might expect that the randomly oriented columnar microstructure should entangle the vortices. Consequently it is somewhat curious that the M_{eq} in polycrystalline materials with random CD's can resemble single crystals with parallel defects. We have suggested¹⁸ that this similarity originates from an anisotropy-induced "refocussing" of the defects and field toward the crystalline c -axis. For highly anisotropic single crystals, it is long recognized that only the normal component of field is effective.¹⁹ More recent studies of polycrystalline Hg-cuprates demonstrated a recovery of vortex variable range hopping (VRH), very similar to that observed in YBaCuO single crystals containing parallel CD's.²⁰ Among the Hg-cuprates with 1, 2, and 3 adjacent Cu-O layers, the recovery of VRH was most pronounced in the Hg-1223 material with the largest mass anisotropy parameter γ . According to the theoretical development, the complexity of randomly oriented columnar defects in a polycrystalline material is reduced to some degree by a large superconducting anisotropy, restoring the simple physics of a crystal with parallel pins. Thus vortex pin-

ning by random CD's provides a reasonable qualitative explanation for the reduction in equilibrium magnetization, despite the complexity of the materials in real space.

Next we use the vortex-defect interaction theory of Wahl et al.¹⁴ to model our experimental data. From the theory, one has

$$M_{eq} = -(\varepsilon_0/2\Phi_0) \times \ln(\beta H_{c2}/B) - (U_0/\Phi_0) \left\{ 1 - \left[1 + \frac{U_0 B_{\Phi}}{\varepsilon_0 B} \right] \exp\left(-\frac{U_0 B_{\Phi}}{\varepsilon_0 B}\right) \right\} \quad (1)$$

where $\varepsilon_0 = [\Phi_0/4\pi\lambda_{ab}]^2$ is the line energy, U_0 is the pinning energy, and $B = (H + 4\pi M) = H$ since M is small. The first term is the conventional London expression. The second is an added term to account for interactions; it is most significant in intermediate fields and it vanishes in large fields $B \gg B_{\Phi}$. In modeling of data at various temperatures T (77, 90, 100, and 110 K), our objective was to maintain an internally consistent set of parameters. The results are shown as solid lines in Fig. 6a for the sample with $B_{\Phi} \sim 1$ T and in Fig. 6b for the sample with a higher defect density. Given the complexity of the polycrystalline material and of the vortex and defect arrays, the description of the experimental data (filled symbols) is relatively good. The values for the pinning energy are a significant fraction of the line energy and are quite reasonable, with $U_0 = 0.65\varepsilon_0$ and $0.8\varepsilon_0$, respectively. To obtain reasonable modeling of the data for the two irradiated materials, we used values of 2.0 and 2.5 T, respectively, for the effective defect densities B_{Φ} . The differences from the nominal values (calculated from the proton fluences) may arise from some overlap of tracks at the highest fluence combined with uncertainty in calculating the production rate for CD's. It is also possible that the effective values for B_{Φ} compensate for other factors, such as residual entanglement and angular distribution in the CD array. Indeed, for more highly anisotropic Tl-2212 materials ($\gamma > 100$, compared with $\gamma \sim 60$ in Hg-1223), similar modeling¹⁸ was achieved with B_{Φ} values within 20% of those calculated from the proton fluence.

An important feature of any superconductor is the London penetration depth. Figure 7 summarizes the results for these materials in a plot of $1/\lambda_{ab}^2$ versus temperature. Values for the virgin sample were obtained from a standard London analysis of the data in Fig. 5. An extrapolation of the Ginzburg-Landau linear dependence near T_c (dashed line) to $T = 0$ yields a value $\lambda(T = 0) = 174$ nm, which is comparable with earlier determinations.²¹ The values for the materials with CD's were obtained from the modeling procedure. All of these results are reasonably behaved, with $1/\lambda_{ab}^2$ varying linearly with T at high temperature. It is clear that proton irradiation increased λ significantly. This is expected, from two theoretical perspectives. First, conventional GLAG theory²² predicts that the penetration depth λ^2 increases as $(1 + \xi_0/\ell)$ when the electronic mean free path ℓ is reduced by scattering, as produced

by irradiation-generated defects from neutrons and secondary protons released by spallation. Second, the theory of Wahl-Buzdin¹⁴ provides that introducing CD's increases the penetration depth as

$$\lambda^{-2}(B_{\Phi}) = \lambda^{-2}(B_{\Phi} = 0) \times [1 - 2\pi R^2 B_{\Phi} / \Phi_0] \quad (2)$$

where R is the radius of the columnar track. The combination of these two effects leads to the significant, progressive increases in λ observed in Fig. 7. To compare with Eq. 2, the inset of Fig. 7 shows $1/\lambda^2$, linearly extrapolated to $T = 0$, plotted versus defect density. The open symbols denote values for B_{Φ} calculated from the proton fluence, while the closed symbols are values used for the modeling, as discussed above. The dashed line in the inset illustrates the theoretical dependence in Eq. 2 and shows a qualitative agreement with the data; its slope corresponds to a value $R \approx 8.4$ nm, somewhat below the 11 nm value obtained for Tl-2212 materials. As discussed previously,¹⁸ it is likely that the CD's have a large effective radius due to oblique passage of ion tracks through CuO planes and a "halo" of oxygen depletion around the central amorphized zone.²³

An interesting consequence of a larger London penetration depth is that the vortex line energy ε_0 decreases significantly. As a result, one can expect the vortex pinning energy of a CD and its pinning force to decrease, reducing its effectiveness. This effect counteracts the nominally positive influence of increasing the defect density B_{Φ} . It is likely that these competing effects play a major role in determining the range of B_{Φ} that maximizes the current density J , as illustrated in the insets of Figs. 2 and 3. This competition is reminiscent of the formation of (point-like) defects in $\text{YBa}_2\text{Cu}_3\text{O}_{7-\delta}$, where progressive removal of oxygen creates defects, but also reduces their effectiveness through increases in the superconductive length scales.^{24,25}

IV. SUMMARY

We irradiated polycrystalline $\text{HgBa}_2\text{Ca}_2\text{Cu}_3\text{O}_x$ materials with 0.8 GeV protons to produce randomly oriented columnar defects via a fission process. Enhancements in vortex pinning increased the persistent current density, with the optimum defect density depending on the range of field and temperature. Adding random linear defects significantly reduced the magnitude of the equilibrium magnetization and changed its dependence on magnetic field from a simple London $\ln(H)$ form (as observed for the virgin material) to a more complex "S-shaped" dependence. Invoking an anisotropy-induced "refocusing" of the vortex-defect array, we have modeled these results using the theory of Wahl-Buzdin that incorporates vortex-defect interactions. This analysis shows that the addition of random columnar defects increases the London penetration depth markedly, which diminishes their effectiveness for pinning vortices. Overall, however, the

formation of randomly oriented columnar defects both enhances the current-carrying performance of the material and creates interesting superconductive systems for study of the interaction of vortices with correlated disorder.

We thank M. Paranthaman for providing the starting Hg-1223 materials used in this study. The work of JGO was supported in part by the Chilean FONDECYT, grant # 1000394. Oak Ridge National Laboratory is managed by UT-Battelle, LLC for the U.S. Department of Energy under contract DE-AC05-00OR22725. Los Alamos National Laboratory is funded by the US Department of Energy under contract W-7405-ENG-36.

V. REFERENCES

-
- ¹ L. Civale, T. K. Worthington, L. Krusin-Elbaum, A. D. Marwick, F. Holtzberg, J. R. Thompson, M. A. Kirk, and R. Wheeler, *J. Metals* **44**, 60-64 (Oct 1992).
 - ² L. Krusin-Elbaum, J. R. Thompson, R. Wheeler, A. D. Marwick, C. Li, S. Patel, D. T. Shaw, P. Lisowski, and J. Ullmann, *Appl. Phys. Lett.* **64**, 3331 (1994).
 - ³ G. W. Schultz, C. Klein, H. W. Weber, B. Moss, R. Zeng, S. X. Dou, R. Sawh, Y. Ren, and R. Weinstein, *Appl. Phys. Lett.* **73**, 3935 (1998) and references therein.
 - ⁴ H. Safar, J. H. Cho, S. Fleshler, M. P. Maley, J. O. Willis, J. Y. Coulter, J. L. Ullmann, P. W. Lisowski, G. N. Riley, M. W. Rupich, J. R. Thompson, and L. Krusin-Elbaum, *Appl. Phys. Lett.* **67**, 130 (1995).
 - ⁵ J. R. Thompson, L. Krusin-Elbaum, D. K. Christen, K. J. Song, M. Paranthaman, J. L. Ullmann, J. Z. Wu, Z. F. Ren, J. H. Wang, J. E. Tkaczyk and J. A. DeLuca, *Appl. Phys. Lett.* **71**, 536 (1997).
 - ⁶ J. R. Thompson, J. G. Ossandon, L. Krusin-Elbaum, K. J. Song, D. K. Christen, J. L. Ullmann, *Appl. Phys. Lett.* **74**, 3699 (1999).
 - ⁷ L. Krusin-Elbaum, G. Blatter, J. R. Thompson, D. K. Petrov, R. Wheeler, J. Ullmann, and C.W. Chu, *Phys. Rev. Lett.* **81**, 3948 (1998).
 - ⁸ L. Krusin-Elbaum, D. Lopez, J. R. Thompson, R. Wheeler, J. Ullmann, C. W. Chu, and Q. M. Lin, *Nature* **389**, 243 (1997).
 - ⁹ Yang Ren Sun, J. R. Thompson, H. R. Kerchner, D. K. Christen, M. Paranthaman, and J. Brynstad, *Phys. Rev. B* **50**, 3330 (1994).
 - ¹⁰ J. A. Lewis, V. M. Vinokur, J. Wagner, and D. Hinks, *Phys. Rev. B* **52**, R3852 (1995).
 - ¹¹ Y. C. Kim, J. R. Thompson, D. K. Christen, Y. R. Sun, M. Paranthaman and E. D. Specht, *Phys. Rev. B* **52**, 4438 (1995).
 - ¹² A. E. Koshelev and V. M. Vinokur, *Phys. Rev. B* **64**, 134518 (2001).

- ¹³ V. G. Kogan, M. M. Fang, and Sreeparna Mitra, Phys. Rev. B **38**, 11958 (1988).
- ¹⁴ A. Wahl, V. Hardy, J. Provost, Ch. Simon, and A. Buzdin, Physica C **250**, 163 (1995).
- ¹⁵ Qiang Li, Y. Fukumoto, Y. Zhu, M. Suenaga, T. Kaneko, K. Sata, and Ch. Simon, Phys. Rev. B **54**, R788 (1996).
- ¹⁶ C. J. van der Beek, M. Konczykowski, T. W. Li, P. H. Kes, and W. Benoit, Phys. Rev. B **54**, R792 (1996).
- ¹⁷ C. J. van der Beek, M. Konczykowski, R. J. Drost, P. H. Kes, N. Chikumoto, and S. Bouffard, Phys. Rev. B **61**, 4259 (2000) and references therein.
- ¹⁸ J. G. Ossandon, J. R. Thompson, L. Krusin-Elbaum, H. J. Kim, D. K. Christen, K. J. Song, and J. L. Ullmann, Supercond. Sci. Technol. **14**, 666 (2001).
- ¹⁹ G. Blatter, V.B. Geshkenbein, and A.I. Larkin, Phys. Rev. Lett. **68**, 875 (1992).
- ²⁰ J. R. Thompson, L. Krusin-Elbaum, L. Civale, G. Blatter, and C. Feild, Phys. Rev. Lett. **78**, 3181 (1997).
- ²¹ J. R. Thompson, “Mercury cuprate high- T_c superconductors: what do their magnetic properties reveal?” in *Studies of High Temperature Superconductors*, vol. **26**, edited by A. V. Narlikar (Nova Science Publishers, Commack, NY, 1998), p. 113-131.
- ²² T. P. Orlando, E. J. McNiff, Jr., S. Foner, and M. R. Beasley, Phys. Rev. B **19**, 4545 (1979).
- ²³ Yimei Zhu, Z. X. Cai, R. C. Budhani, M. Suenaga, and D. O. Welch, Phys. Rev. B **48**, 6436 (1993).
- ²⁴ J. G. Ossandon, J. R. Thompson, D. K. Christen, B. C. Sales, H. R. Kerchner, J. O. Thomson, Y. R. Sun, K. W. Lay, and J. E. Tkaczyk, Phys. Rev. B **45**, 12534 (1992).
- ²⁵ J. G. Ossandon, J. R. Thompson, D. K. Christen, B. C. Sales, Yang Ren Sun, and K. W. Lay, Phys. Rev. B **46**, 3050 (1992).

FIGURE CAPTIONS

Fig. 1. The magnetization of polycrystalline Hg-1223 materials at 60 K, versus applied magnetic field. Samples were irradiated with various fluences ϕ_p of 0.8 GeV protons, as shown, to create randomly oriented columnar defects with approximate “matching fields” B_Φ .

Fig. 2. The intra-granular persistent current density J vs temperature for various irradiated materials, measured in applied magnetic field of 0.1 T. The inset shows that J at 100 K is maximized at a defect density of 0.1–0.3 T.

Fig. 3. The intra-granular persistent current density J vs temperature for various irradiated materials, measured in applied magnetic field of 1 T. Inset: J at 60 K versus defect density B_Φ exhibits a maximum at a defect density of ~ 2 T.

Fig. 4. The magnetization of virgin Hg-1223 at 77 K, versus applied magnetic field (log scale). Open squares show the measured M in increasing and decreasing field history, while closed squares show the average $M \approx M_{eq}$. The solid line is a fit to the conventional London $\ln(H)$ dependence. Data for Hg-1223 containing randomly oriented columnar defects are included for comparison.

Fig. 5. The equilibrium magnetization $M_{eq}(H, T)$ plotted vs $\ln(H)$ for unirradiated Hg-1223 at the tem-

peratures shown. Lines are fits to conventional London theory.

Fig. 6. Plots of $M_{eq}(H, T)$ vs. $\ln(H)$ for irradiated Hg-1223 with (a) $B_\Phi \sim 1$ T and (b) with $B_\Phi \sim 3.4$ T. Symbols are experimental results, while lines show modeling of data using Eq. 1 where effects of vortex-defect interactions are included.

Fig. 7. The temperature dependence of the London penetration depth $1/\lambda^2$. Values for the virgin sample come from a conventional London analysis of the data in Fig. 5; for the irradiated materials, values come from modeling the equilibrium magnetization shown in Fig. 6. Inset shows values for $1/\lambda^2$, extrapolated to $T = 0$, plotted versus defect density; open symbols denote B_Φ values calculated from the proton fluence and closed symbols are values used in the modeling.

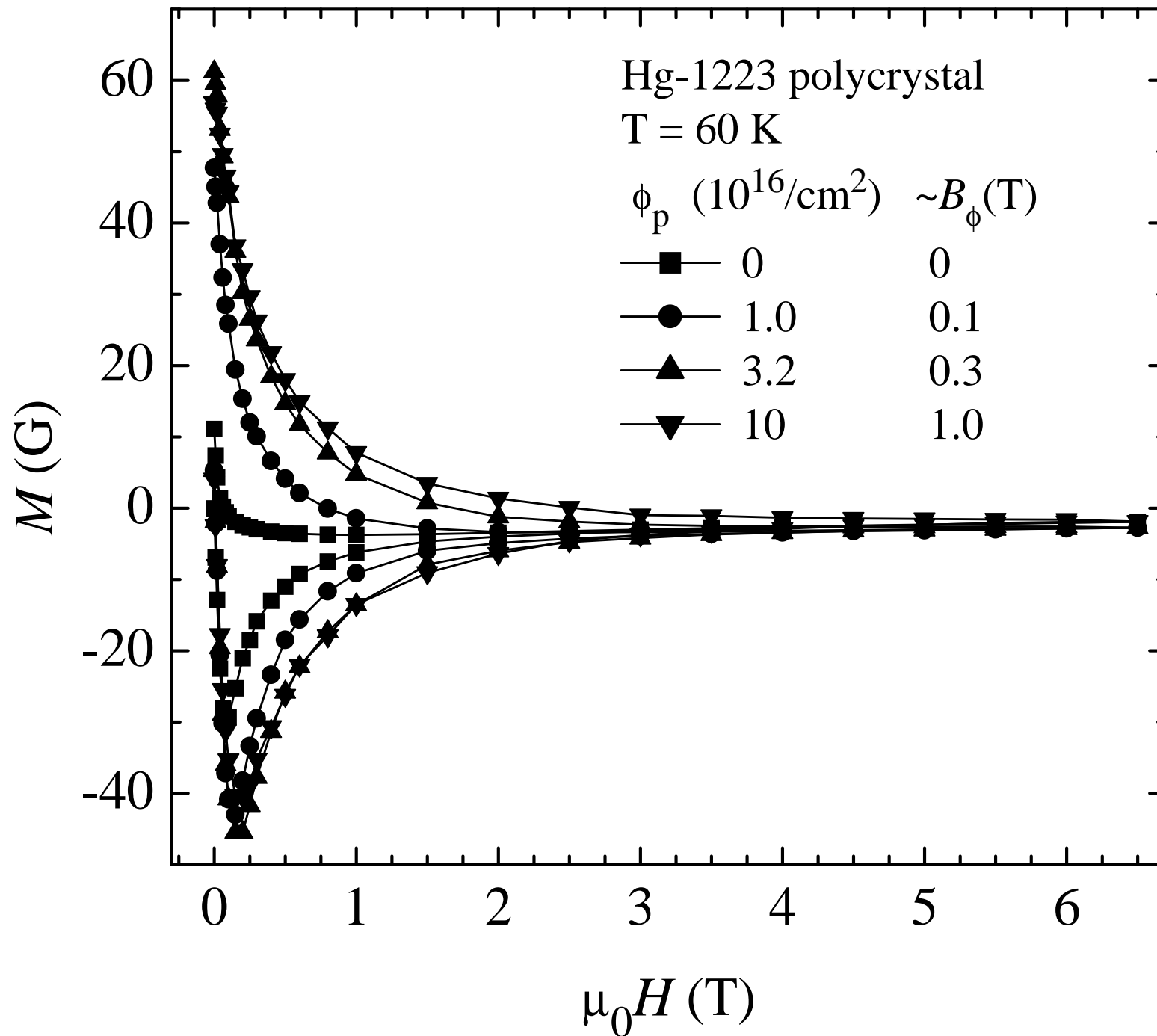


Fig. 1: JR Thompson et al.

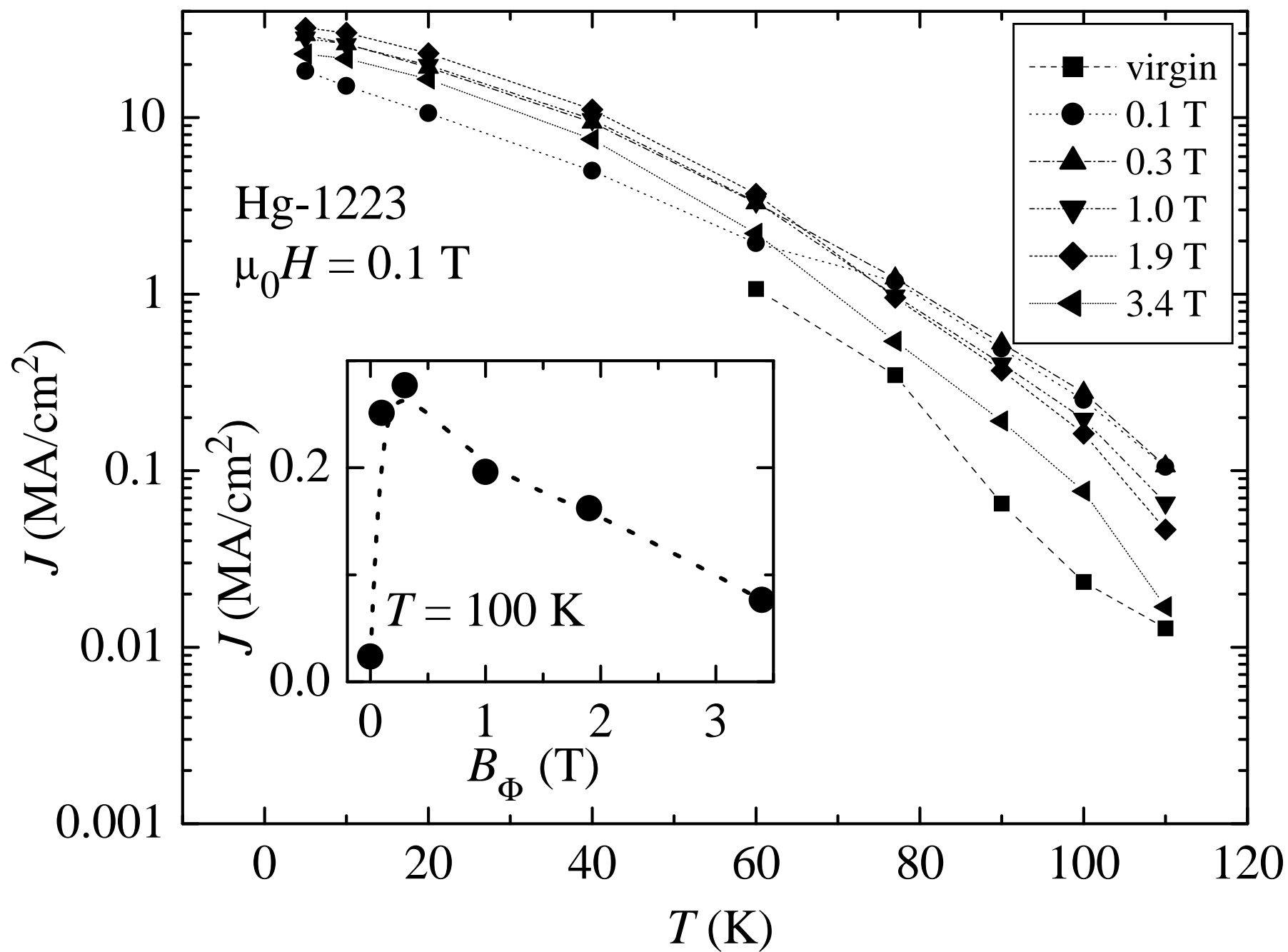


Fig. 2: JR Thompson et al.

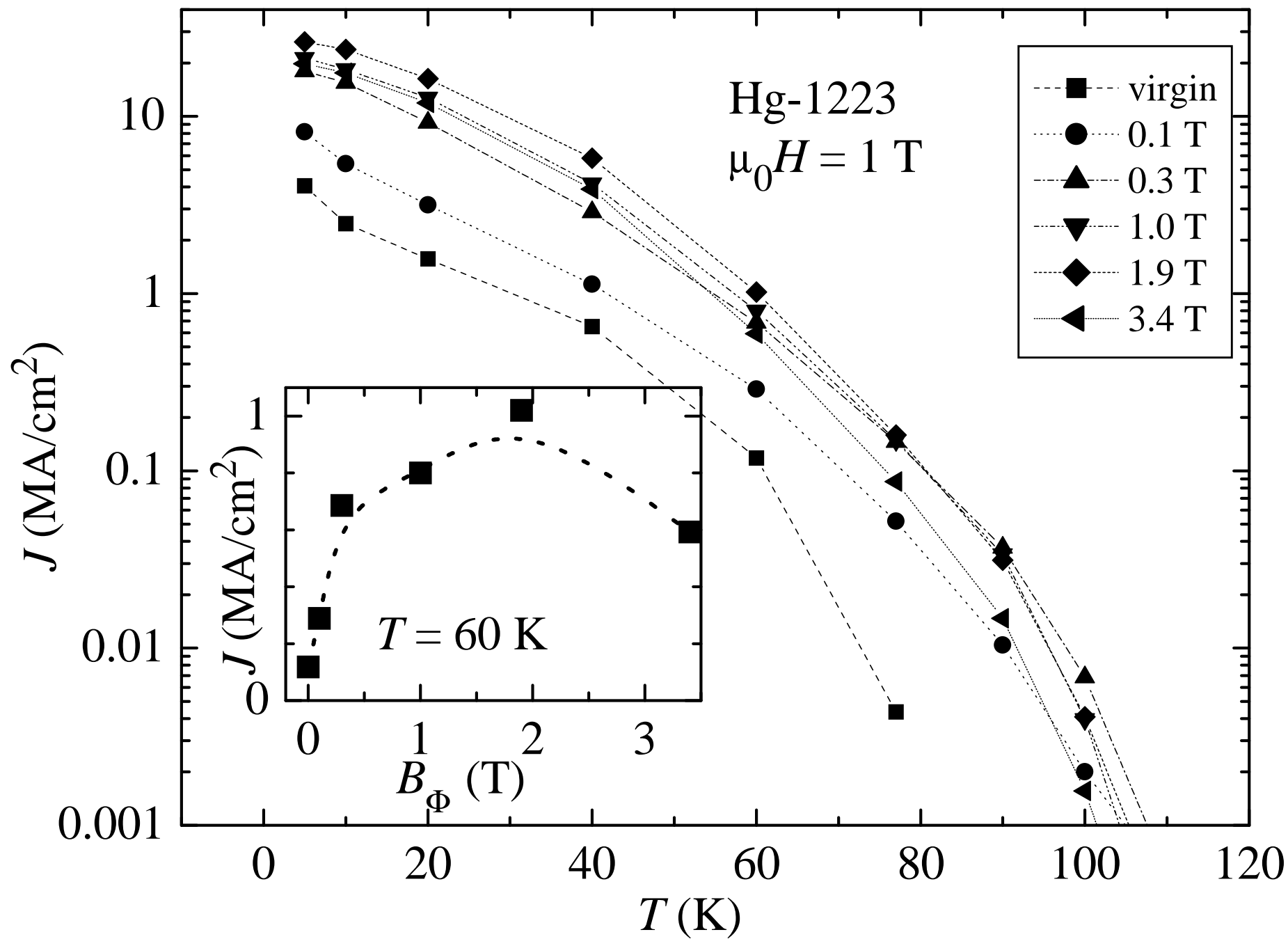


Fig. 3: JR Thompson et al.

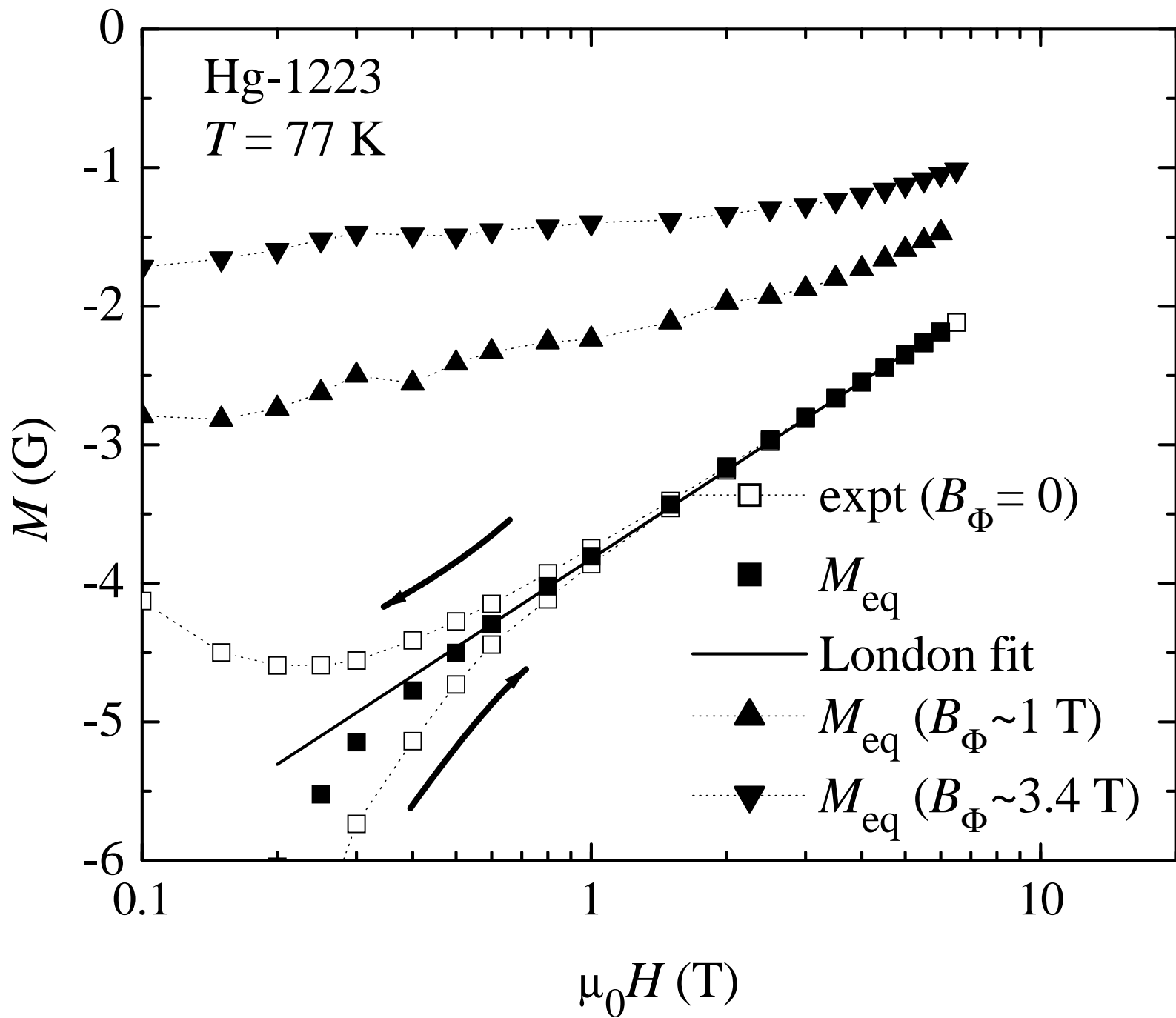


Fig. 4, Thompson

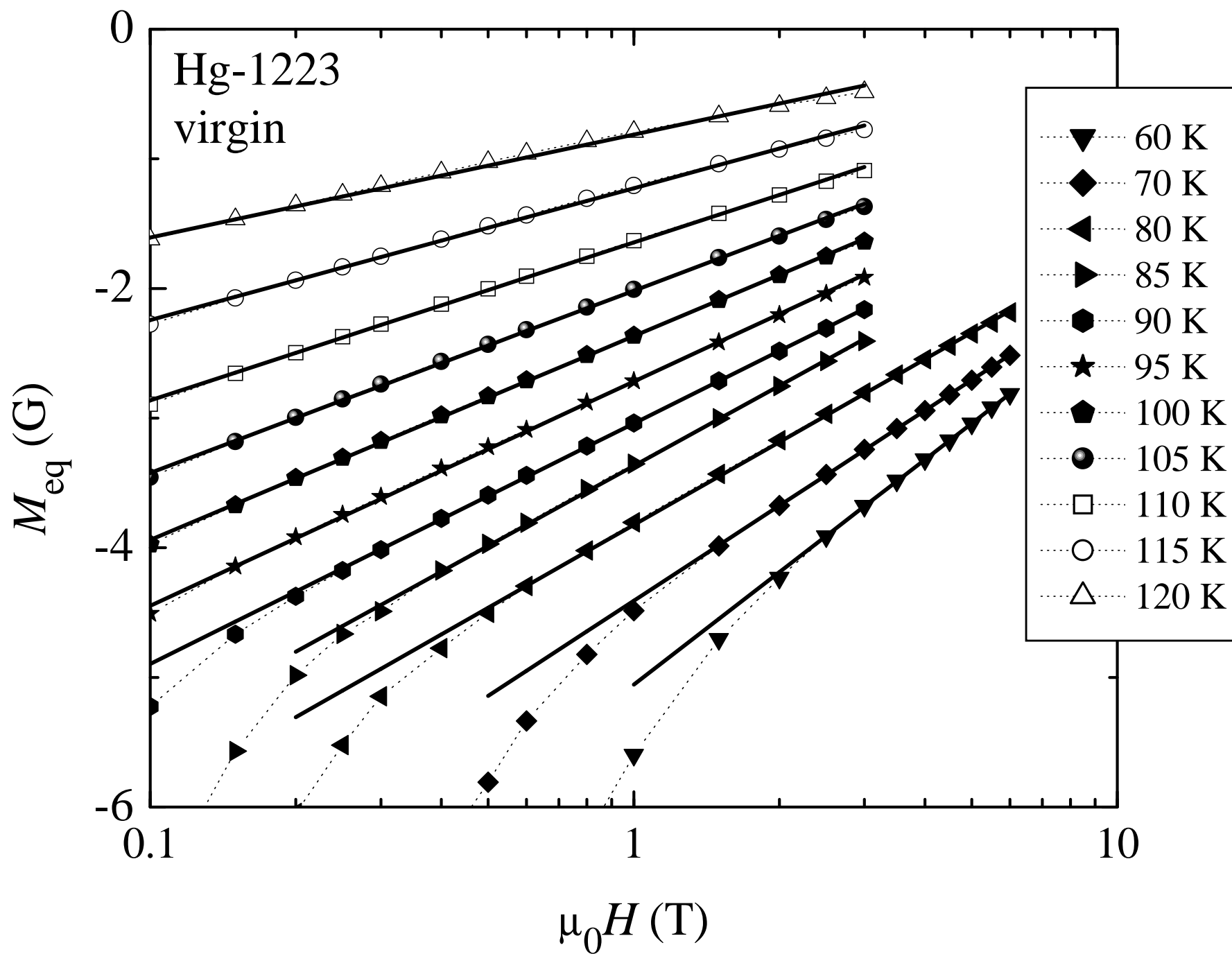


Fig. 5: JR Thompson et al.

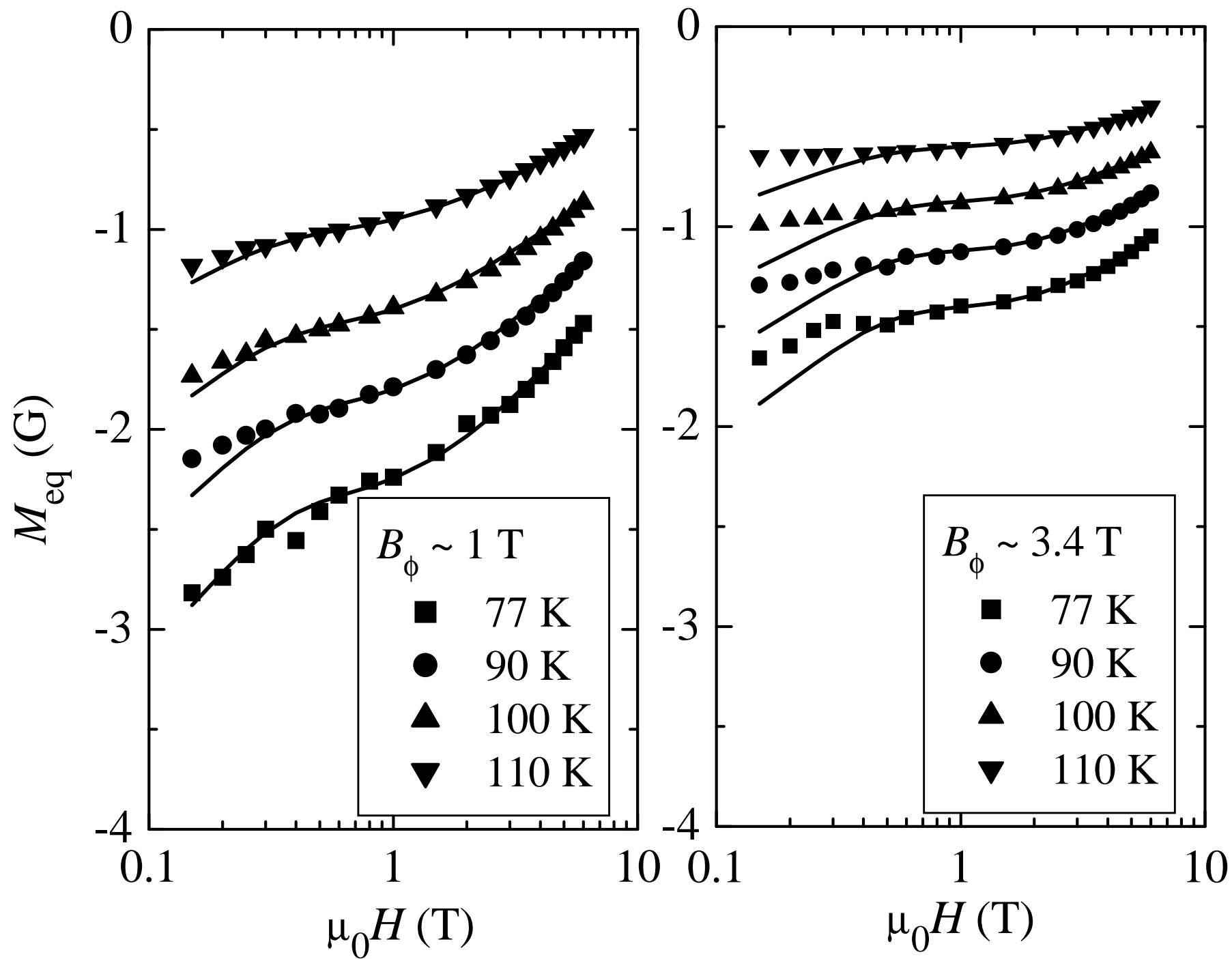


Fig. 6: JR Thompson et al.

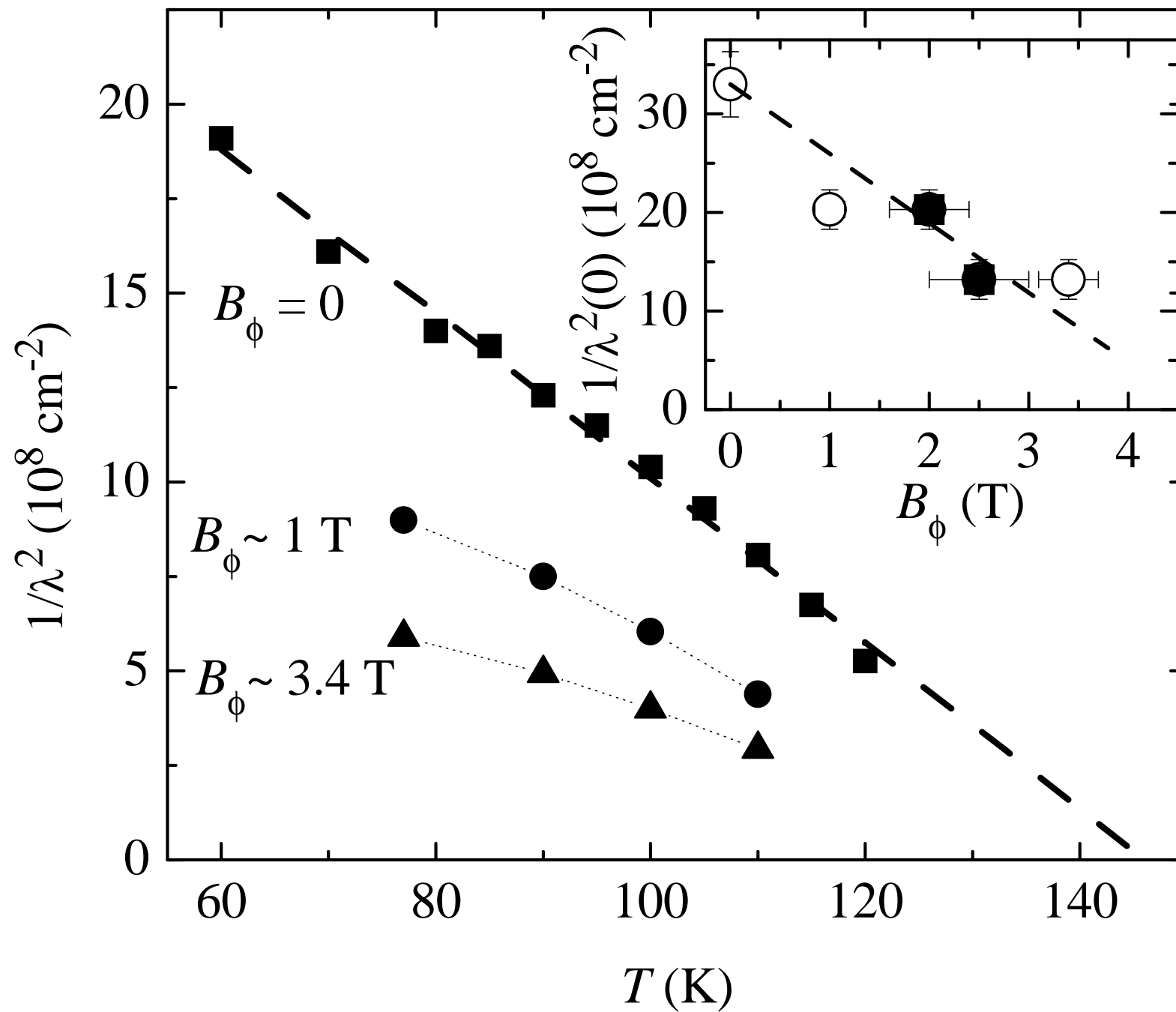


Fig. 7: JR Thompson et al.